

FAST AND ROBUST GAUSSIAN MIXTURE MODEL FOR MRI BRAIN IMAGE SEGMENTATION

M.A. Balafar

*Department of IT, Faculty of Electrical and Computer Engineering, University of Tabriz, Tabriz, Iran
balafarila@tabrizu.ac.ir*

Abstract- Image segmentation is crucial and preliminary stage of almost all medical imaging diagnosis tools. Gaussian Mixture Model (GMM) is one of common methods for image segmentation and usually, Expectation Maximizing (EM) is used to estimate the parameters of this model. In order to improve EM performance in presence of noise, an extension for EM is proposed which incorporates mean-filtered image as neighborhood information in clustering. In addition, the histogram of image is used as input for clustering to speed up the process. Proposed algorithm quantitatively evaluated in compare to current extensions for EM.

Keywords: Clustering, Brain, MRI, Expectation Maximizing (EM).

I. INTRODUCTION

Medical images almost are stored and represented digitally [1]. Data acquisition, processing and visualization techniques facilitate diagnosis. There are different medical image types such as ultrasound images, X-ray computed tomography, digital mammography, Magnetic Resonance Image (MRI), and so on [2].

MRI images widely are used by researchers in medical image processing. Magnetic resonance imaging (MRI) is an important imaging technique for the detecting abnormal changes in different part of brain in early stage. MRI imaging is popular to obtain image of brain with high contrast. MRI acquisition parameters can be adjusted to give different grey level for different tissues and various types of neuropathology [3]. The brain images segmentation is a complicated and challenging task due to noise and inhomogeneity [4, 5]. However, accurate segmentation of these images is very important for detecting tumors, edema, and necrotic tissues. Accurate detecting of these tissues is very important in diagnosis systems. Many techniques have been used for image segmentation [6], like thresholding, region growing, statistical models, active contour models and clustering [7, 8, 9]. The distribution of intensities in medical images is usually very complex, and therefore, determining of threshold is difficult and thresholding methods fail in these images. Mostly, thresholding method is combined with other methods. Region growing method

extends thresholding by combining thresholding with connectivity. This method needs seed for each region and have the same problem of thresholding for determining suite threshold for homogeneity [10]. There are many segmentation algorithms [11] but there is not a generic algorithm for totally successful segmentation of medical images.

Clustering algorithms are popular segmentation methods which classify feature vectors into clusters such that in-cluster vectors are more similar to each other than vectors in different clusters. The fuzzy c-means (FCM) algorithm [10, 11, 14] and the Gaussian mixture model (GMM) [15] are popular clustering methods. Both of them obtain class probability distributions and yield soft segmentation. The fuzzy c-means attempt to minimize inside cluster distance and don't use intensity distributions. Gaussian mixture model uses the statistical theory to cluster input image and usually, EM is used to estimate the parameters of this model. Both of these methods just consider intensity of image and in noisy images, intensity is not trustful. Therefore, this algorithm has not good result in noisy images.

In order to overcome noise problem, many researchers attempted to incorporate spatial information in image classification methods such as FCM and GMM. Zhang et. Al. [16] proposed a novel Gaussian hidden Markov random field (HMRF) model to integrate spatial information into Gaussian model. They used a Markov Random Field-Maximum A Posteriori (MRF-MAP) approach to estimate model solution. Tang et al. [17] proposed a neighborhood weighted Gaussian mixture model to overcome misclassification on the boundaries and inhomogeneous regions of MRI brain images with noise. Expectation maximization algorithm is used as optimization method. In this paper, a new extension for EM is proposed which in a new way incorporates neighborhood information in Gaussian mixture model.

II. BACKGROUND

The Gaussian mixture model has K mixed component densities (Gaussian distribution) with K mixing coefficients. Each component is assigned to one target class and the goal is to obtain the class probabilities of each voxel. The probability distribution of the k th

component is denoted by $p_k(x|\theta_k)$, where x is input image and θ_k is the parameters of component k . The probability of each voxel can be described as a mixture of probability distributions as follows:

$$p(x|\theta) = \sum_{k=1}^K \alpha_k p_k(x|\theta_k) \quad (1)$$

where α_k denotes the mixture coefficients with the constraint that $\sum_{k=1}^K \alpha_k = 1$. The probability distribution of component k is modeled by a Gaussian distribution with mean μ_k and covariance matrix Σ_k :

$$p_k(x|\theta_k) = p_k(x|\mu_k, \Sigma_k) = \frac{1}{\sqrt{\det(2\pi\Sigma_k)}} e^{-(x-\mu_k)^T \Sigma_k^{-1} (x-\mu_k)/2} \quad (2)$$

Usually, ML estimation is used to find the parameters. The log-likelihood expression for the parameters θ and the data X is defined as follow:

$$\log(L(\theta|X)) = \log \prod_{i=1}^N p(x_i|\theta) = \sum_{i=1}^N \log \left(\sum_{j=1}^k \alpha_j^t p_j(x_i|\theta_j^t) \right) \quad (3)$$

Finding the ML solution from this equation is difficult. Usually, the expectation maximization (EM) is used to obtain the parameters. The EM steps are demonstrated in the following list:

- Initialization: mean and covariance matrix are initialized using k -means and prior probability is initialized uniformly $P_i = 1/L$.
- E-step: calculate membership probability of each data.
- M-step: compute mean and variance of each Gaussian component using Membership Probability obtained in E-step.
- EM steps are repeated until convergence.
- Bayes' rule is used to obtain the probability of each data (E-step):

$$p(k|x_i, \theta^t) = \frac{\alpha_k^t p_k(x_i|\theta_k^t)}{\sum_{j=1}^k \alpha_j^t p_j(x_i|\theta_j^t)} \quad (4)$$

Probability obtained in E-step is used to obtain mixing coefficient, mean and covariance matrix (M-step):

$$\alpha_k^{t+1} = \frac{1}{N} \sum_{i=1}^N p(k|x_i, \theta^t) \quad (5)$$

$$\mu_k^{t+1} = \frac{\sum_{i=1}^N x_i p(k|x_i, \theta^t)}{\sum_{i=1}^N p(k|x_i, \theta^t)} \quad (6)$$

$$\Sigma_k^{t+1} = \frac{\sum_{i=1}^N p(k|x_i, \theta^t) \cdot (x_i - \mu_k^{t+1})(x_i - \mu_k^{t+1})^T}{\sum_{i=1}^N p(k|x_i, \theta^t)} \quad (7)$$

The GMM doesn't contain any spatial information. One of important spatial information is the neighborhood of pixels (voxels). Using the neighborhood information can improve the classification result. The GMM obtains the class probabilities based on intensity of pixels (voxels) without considering any neighborhood information. Hui Tang et al. [17] proposed a neighborhood weighted Gaussian mixture model. They considered the fact that usually the tissues are continuous and it is reasonable to consider the probability of the k th class is affected by k th class probabilities of the neighbors. They defined the neighborhood weighted probability for the current pixel as follow:

$$p(k|x_i, \theta^t) = \frac{\alpha_k^t W_{ik}^t p_k(x_i|\theta_k^t)}{\sum_{j=1}^k \alpha_j^t p_j(x_i|\theta_j^t)} \quad (8)$$

where W_{ik} is the average probability of belonging neighborhood of pixel i to class k and is defined as follow:

$$W_{ik} = \frac{\sum_{r \in N_i} p(k|x_r, \theta^t)}{N_i} \quad (9)$$

where N_i denotes the set of neighbors which determined by a window centered on x_i .

III. METHODOLOGY

In this section, a new extension for EM which use average image as input for clustering is proposed. Proposed algorithm uses the histogram of image as input for clustering to speed up the clustering process.

A. New Extensions for EM

In order to speed up the clustering process for input image, instead of using neighborhood information in iteration process, average image is used as input for clustering. Clustering based on proposed algorithm is called EM-E.

Image averaging reduces noise but has degrading effects such as blurring. In low level of noise, image degrading effect is more than noise reduction effect and clustering of original image produces better results than clustering of average image. In order to overcome this shortcoming, a threshold based on variance of noise is used to tradeoff between original image and average image. Threshold value of 3 is used which is obtained by error and trial. In this algorithm, the \bar{x}_i average of neighbor pixels around pixel x_i is calculated prior to clustering. Then a linearly-weighted sum of \bar{x}_i and x_i is used as input for clustering:

$$o_i = (1-\beta)x_i + \beta\bar{x}_i \quad (10)$$

where o_i represents the value of pixel i in generated image which is used as input for clustering. The parameter β determines the weight of neighborhood information. We set its value to $(\sigma-2)$, where σ is the variance of noise. This value is obtained using error and trial.

In MRI, noise is Rician distributed [18]. Noise distribution approaches Gaussian with increasing Signal to Noise Ratio (SNR) and approaches Rayleigh with decreasing SNR [18]. Rician distribution in background is Rayleigh because there is no signal in background. The Rayleigh PDF of the statistically independent observations is

$$p(\{O_i\}) = \prod_{i=1}^n \frac{O_i}{\sigma^2} e^{-(O_i^2)/(2\sigma^2)} \quad (11)$$

where O is observations and σ^2 is the variance of noise. The variance is calculated by maximizing the log-likelihood of PDF function with respect to variance:

$$\sigma_{Noise}^2 = \frac{1}{2n} \sum_{i=1}^n O_i^2 \quad (12)$$

In order to speed up clustering process, the grey-level histogram of the sum image O is used as input for clustering. In the likelihood function (Equation (4)), the distribution value of pixels is replaced with multiplication of the distribution value of each grey level on number of pixels with that grey level as follow:

$$\begin{aligned} \log(L(\theta | I)) &= \log \prod_{i=1}^q p(g_i | \theta) = \\ &= \sum_{i=1}^q \log \left(\sum_{j=1}^k \alpha_j^t f_i^* p_j(k | g_i, \theta_j^t) \right) \end{aligned} \quad (13)$$

where g_i denotes i th grey value in histogram, f_i is the number of the pixels with the grey value g_i , θ_j^t represents the parameters of the j th cluster at t iteration, and q represents the number of the grey levels of the histogram which is much smaller than the number of pixels in the image. The EM steps are modified as follow:
a. In Equation (6), the value of pixels is replaced with multiplication of the value of each grey level (g_i) on number of pixels with that grey level (f_i) as follow:

$$\mu_k^{t+1} = \frac{\sum_{i=1}^N g_i * f_i * p(k | g_i, \theta^t)}{\sum_{i=1}^N f_i * p(k | g_i, \theta^t)} \quad (14)$$

b. In Equation (7), the distance of pixels from component centre is replaced with multiplication of the distance of each grey level (g_i) from center of component (μ_k) on number of pixels with that grey level (f_i) to form an equation as follow:

$$\sum_k^{t+1} = \frac{\sum_{i=1}^N p(k | g_i, \theta^t) * (f_i * (g_i - \mu_k^{t+1})(g_i - \mu_k^{t+1})^T)}{\sum_{i=1}^N (f_i * p(k | g_i, \theta^t))} \quad (15)$$

B. Improve Clustering Results Using User Interaction

Sometimes, due to in-homogeneity, low contrast, noise and inequality of content with semantic, automatic methods fail to segment image correctly. Therefore, for these images, it is necessary to use user interaction to

correct method's error. However, robust semi-automatic methods can be developed in which user interaction is minimized.

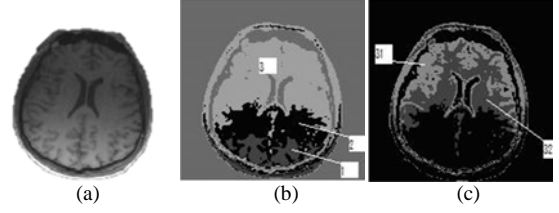


Figure 1. (a) A real brain image, (b) its 4 clusters, (c) two sub clusters of Cluster 3

Sometimes, clustered image, for example in Figure 1(b), either has two or more target class in one cluster (white matter and grey matter of brain in cluster number 3) or one target class in two or more clusters (white matter in clusters number 1, 2 and 3). For solving this problem, user selects clusters contain several classes (cluster number 3) to be partitioned again, afterwards, each user selected cluster is re-clustered to two sub clusters. Figure 1(c) demonstrates sub clusters of class number 3. The cluster number 3 is clustered to two sub clusters number 31 and 32.

This process continues until user is satisfied. That means quality of segmentation depends on user. Then, to solve problem of several clusters for one class, user selects clusters for each target class (clusters 1, 2 and sub cluster 32 are selected for white matter).

IV. RESULTS AND DISCUSSION

The proposed extension of EM (EM-E) is simulated and applied on the simulated images from BrainWeb [19] and real images from Internet Brain Segmentation Repository (IBSR) [20]. The results of proposed algorithm are compared with reported results for the existing extensions of EM [21] (DPM, rjMCMC, KVL, MPM-MAP), existing neighborhood based extension for EM (NWEM [17]) reported results in IBSR, existing neighborhood based extension for FCM (FCM_S [22], FGFCM [23], FCM_EN [24] and NonlocalFCM [25]) and other published results.

The results of algorithms are compared quantitatively to analyze their performance. The similarity index is used to evaluate the algorithms quantitatively. The similarity index, ρ is the degree of matching between ground truth and segmentation result. It is defined as

$$\rho = \text{avg} \left(\frac{2 |X_i + Y_i|}{|X_i| + |Y_i|} \right) \quad (16)$$

where X_i represents class i in ground truth and Y_i represents the same class in the segmentation result.

A. Simulated Images

The simulated MRI images are obtained from BrainWeb. A simulated data volume with T1-weighted sequence, slice thickness of 1 mm and a volume size of $217 \times 181 \times 181$ is used. Non-brain tissues are removed prior to segmentation.

The number of tissue classes in the segmentation is set to three: grey matter (GM), white matter (WM) and cerebrospinal fluid (CSF). Mind that background pixels are ignored in this experiment.

First, proposed segmentation algorithm (EM-E) and NWEM are compared. They are applied on brain image from BrainWeb corrupted by different noise levels. Figure 2 shows the segmentation results of applying EM-E and NWEM on 90th slice of the image with 9% Rician noise. Figure 2(a) is noisy image. Figure 2(b) is ground truth. Figure 2(c) is the segmentation result of EM-E. Figure 2(d) is the segmentation result of NWEM. In Figure 2, it is not difficult to find that NEWM is more influenced by the noise in comparison with EM-E, in which fewer artifacts is evident, resulting in clear segmentation result.

The similarity index of segmentation results is used to evaluate algorithm quantitatively. The similarity index, ρ of segmentation results in Figure 2, is presented in Figure 4. The Figure 4 shows that even for the image with 9% noise, the similarity indices ρ in EM-E is larger than 92%. The quantitative evaluation supports the achieved conclusion for the qualitative results.

Figure 3 shows the same results on a slice with 7% Rician noise as well as it shows that segmentation result of EM-E is clear. Figure 3 also shows that segmentation result of NWEM is more influenced by noise. EM-E produced clear segmentation result and is more convincing in segmentation. The following quantitative evaluation supported the achieved conclusion.

The similarity index, ρ of segmentation result in Figure 3 is presented in Figure 4. Figure 4 shows that EM-E produces similarity index higher than NWEM. EM-E exhibited more robustness to noise. Then, in order to compare performance of proposed algorithm (EM-E) on 3D image volumes, EM-E and neighborhood based extensions for EM are applied to brain image volume and average similarity value is used to evaluate them.

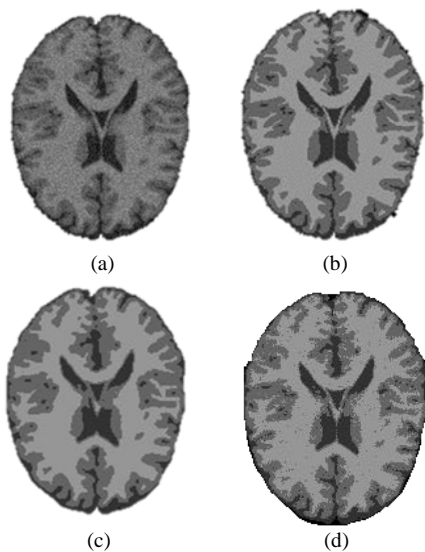


Figure 2. The segmentation results of applying proposed algorithm on a slice of the image with 9% Rician noise, (a) Noisy image; (b) Ground truth; Segmentation results of (c) EM-E; (d) Segmentation results of NWEM

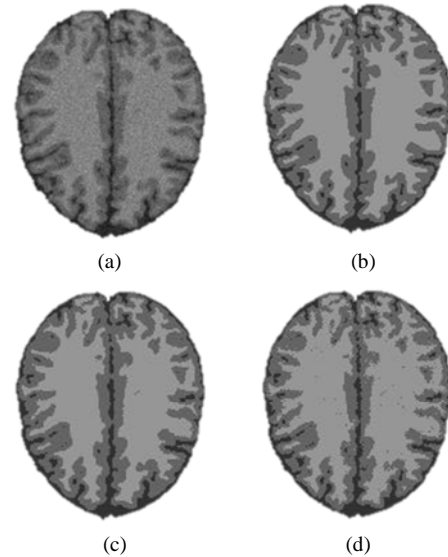


Figure 3. The segmentation results of applying proposed algorithm (EM-E) on a slice of the image with 7% Rician noise, (a) Noisy image; (b) Ground truth; Segmentation results of (c) EM-E; (d) Segmentation results of NWEM

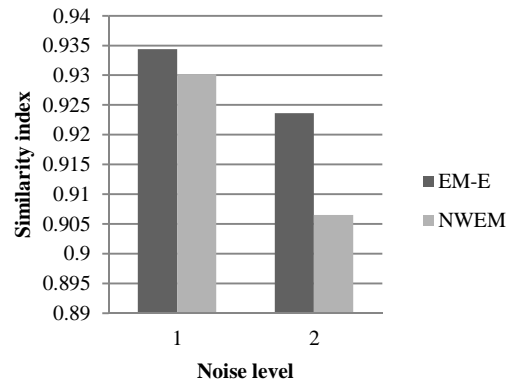


Figure 4. Similarity index ρ of segmentation results in Figures 2 and 3

Figure 5 shows the average similarity indices ρ for EM-E and EM extensions (DPM, rjMCMC, KVL, MPM-MAP and NWEM) when they are applied on 3D volume in different noise levels. MPM-MAP is an atlas-based modified Gaussian and MRF model. EM-E gave results comparable with the best reported results, in low levels of noise. For noise levels more than 5%, EM-E outperformed other competing algorithms and this difference in performance increases at 9% noise level. When the noise level is increased, the similarity indices of EM-E decrease more slowly than others.

EM-E is also compared with neighborhood based extensions for FCM. Figure 6 shows the average similarity indices ρ for EM-E, FCM extensions (FCM-S, FCM-EN, FGFCM, NonlocalFCM), and TODAS [26] (topology-preserving anatomy-driven segmentation) when they are applied on 3D volume in different noise levels. At the 3% noise level, the results for the proposed segmentation algorithm and the best reported results were close. Above 3% noise levels, EM-E produced higher similarity indices and were the most convincing in segmentation. The superiority of these algorithms increased with increment in noise levels.

In [27], Re-FC (combination of fuzzy connectedness and inhomogeneity correction) is applied on brain MRI volumes from Brainweb with 3% noise. Average similarity index for this algorithm is 0.9. EM-E is applied on the same images. Average similarity index is 0.9612.

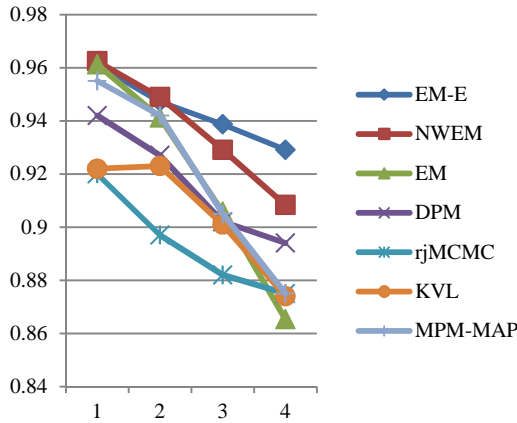


Figure 5. Average similarity indices ρ for different noise levels

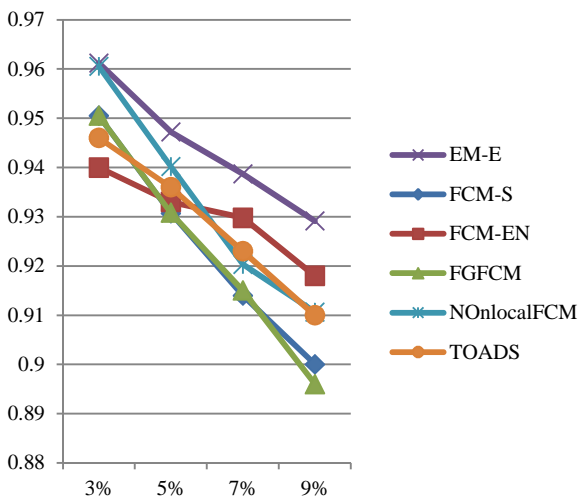


Figure 6. The average similarity indices ρ for EM-E and FCM extensions in different noise level

Afterwards, proposed algorithm with different neighborhood sizes are applied on 3D volume and average similarity is used to analyze the effect of different neighborhood sizes on performance of proposed algorithm. Figure 7 shows the average similarity index ρ of proposed algorithm when with different neighborhood sizes is applied on the simulated image with 9% noise. Figure 7 shows that when the neighborhood size is increased, the similarity indices of the algorithm decrease.

B. Real Images

The superiority of proposed algorithm is also demonstrated on real MRI images. The real MRI images are obtained from the IBSR by the Centre for Morphometric Analysis, Massachusetts General Hospital. 20 normal data volume with T1-weighted sequence are used.

In IBSR, manual segmentation results are provided along with brain MRI data to encourage introducing new segmentation algorithms and evaluate their performance. Trained investigators used semi-automated histograms on the spatially normalized images to obtain manually segmentation.

In order to compare proposed algorithm and NWEM on different image qualities, the proposed algorithms are applied to all 20 normal real MRI volumes and average similarity index ρ of them is used to provide quantitative results. Figure 8 shows the average similarity index values of two algorithms for all 20 normal images. The Figure 8 shows that proposed algorithm produces the average similarity indices ρ higher than NWEM.

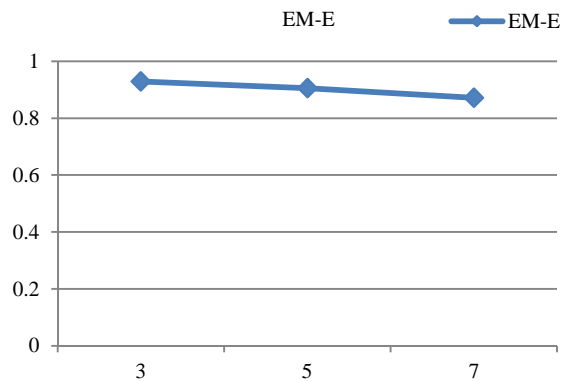


Figure 7. Average similarity index ρ for different neighborhood sizes on simulated image with 9% noise

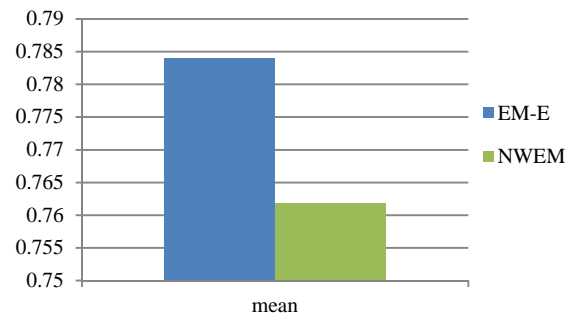


Figure 8. Average similarity index of proposed algorithm when applied on 20 real images

The average similarity index values of proposed algorithm for 20 normal real MRI volumes and reported results in IBSR are compared. Figure 9 shows the average similarity index values of different algorithms for all 20 normal images. Figure 9 shows that proposed algorithm produces the average similarity indices ρ higher than other algorithms and near to manual results, meaning that the proposed algorithm produced more accurate segmentation result.

In [28], DPM and MPM-MAP are applied on first 13 volumes from IBSR. Average similarity index for these algorithms are 0.7006 and 0.6538. EM-E is applied on the same images. Average similarity index is 0.7650. In [27], Re-FC is applied on 20 volumes from IBSR. Average similarity index for this algorithm is 0.722. The EM-E is applied on the same images. Average similarity index is 0.7715.

The EM-E is also compared with neighborhood based extensions for FCM. Figure 10 shows the average similarity indices ρ for EM-E and FCM extensions (FCM-S1, FCM-EN, FGFCM) for all 20 normal images. Figure 10 shows that EM-E produces highest similarity indices and outperformed other methods.

At last, the effect of user-interaction on clustering results is investigated. EM-E (proposed algorithm) and the same algorithm with user-interaction are applied to all 20 normal real MRI volumes and similarity index ρ is used to compare the segmentation results, quantitatively. The average similarity index values of two algorithms for different image were presented in Figure 11. The Figure 11 shows that EM-1 with user-interaction produces higher or almost equal similarity indices ρ .

Figure 12 shows the average similarity index values of two algorithms for all 20 normal images. Figure 12 shows that user-interaction improves the performance of EM-1 algorithm and EM-1 with user-interaction produces higher average similarity indices ρ .

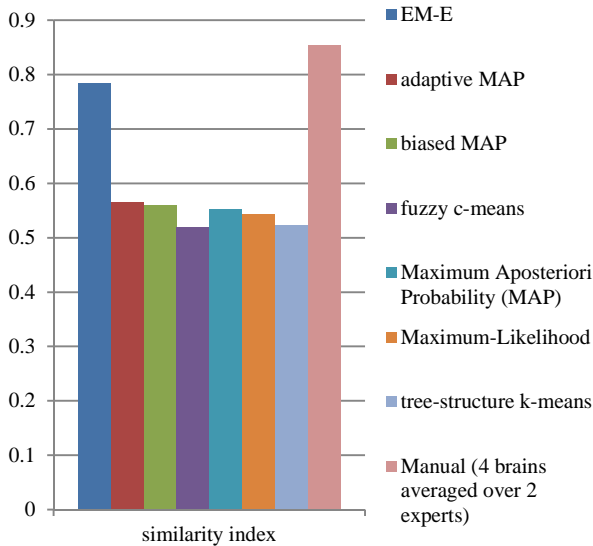


Figure 9. Average similarity index of different algorithms when applied on 20 real images

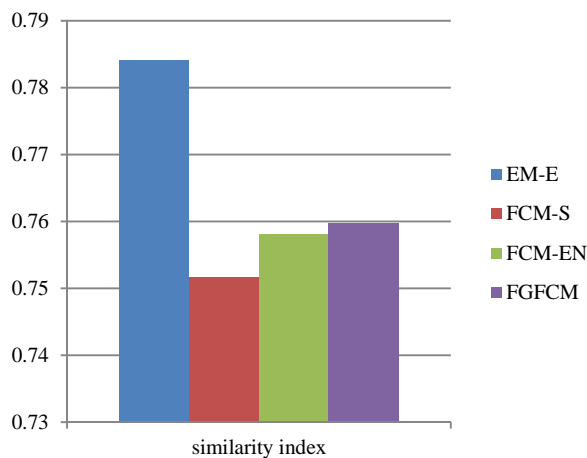


Figure 10. Average similarity index of proposed algorithm and neighborhood based FCM extensions when applied on 20 real images

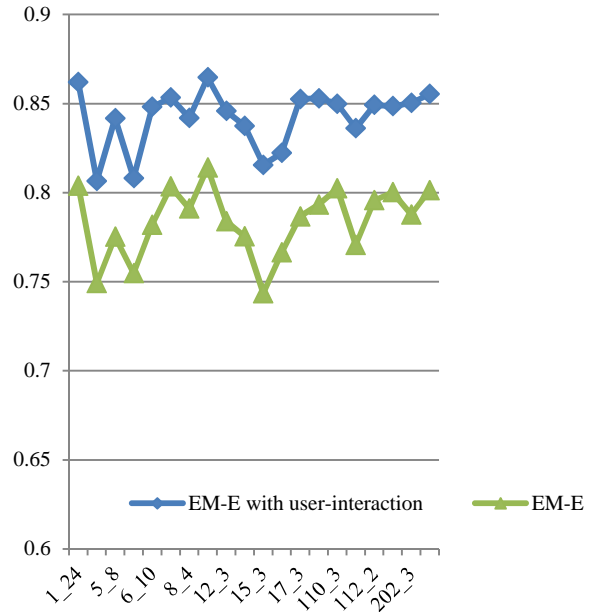


Figure 11. Similarity index of different algorithms when applied on 20 real images

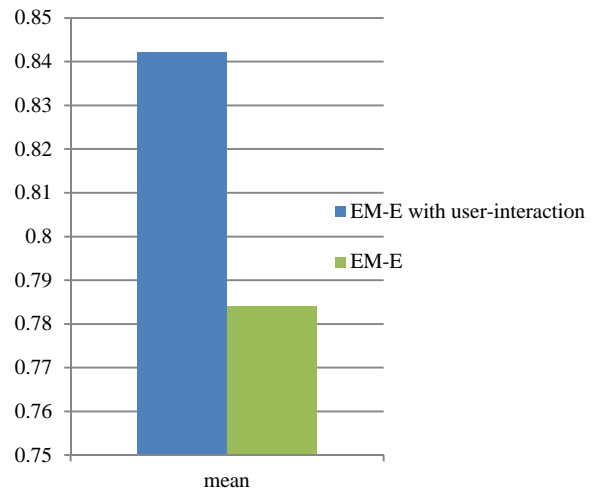


Figure 12. Average similarity index of proposed algorithm when applied on 20 real images

V. CONCLUSIONS

Researchers widely use clustering methods for medical image segmentation. FCM and EM are popular clustering methods. Traditional clustering methods just consider intensity information and have not good results in presence of noise. Using spatial information is one solution to overcome this problem. In this paper, an extension for EM is proposed. In proposed algorithm, neighborhood information in a new way is incorporated in clustering process. In order to overcome the problem of standard EM in presence of noise, introduced algorithm use average image as input for clustering. In order to speed up clustering process, the histogram of image is used as input for clustering. The similarity index is used to evaluate different algorithms. Experimental results demonstrate the superiority of introduced algorithm.

REFERENCES

- [1] P.L. Chang, W.G. Teng, "Exploiting the Self-Organizing Map for Medical Image Segmentation", *CBMS*, pp. 281-288, 2007.
- [2] J. Jan, "Medical Image Processing Reconstruction and Restoration Concepts and Methods", Taylor and Francis, CRC, 2005.
- [3] D. Tian, L. Fan, "A Brain MR Images Segmentation Method Based on SOM Neural Network", *ICBBE*, pp. 686-689, 2007.
- [4] M.A. Balafar, "Review of Noise Reducing Algorithms for Brain MRI Images", *International Journal on Technical and Physical Problems of Engineering (IJTPE)*, Issue 13, Vol. 4, No. 4, pp. 54-59, December 2012.
- [5] M.A. Balafar, "Review of Intensity Inhomogeneity Correction Methods for Brain MRI images", *International Journal on Technical and Physical Problems of Engineering (IJTPE)*, Issue 13, Vol. 4, No. 4, pp. 60-66, December 2012.
- [6] M.A. Balafar, A.R. Ramli, M.I. Saripan, S. Mashohor, "Review of Brain MRI Image Segmentation Methods", *Artificial Intelligence Review*, Vol. 33, No. 33, pp. 261-274, 2010.
- [7] A. Banakar, M. Fazle Azeem, "Artificial Wavelet Neuro-Fuzzy Model Based On Parallel Wavelet Network and Neural Network", *Soft Computing*, Springer, Vol. 12, No. 8, pp. 1463-1485, 2008.
- [8] M. O'Neill, A. Brabazon, "Self Organising Swarm (SOSwarm)", *Soft Computing*, Springer, Vol. 12, No. 11, pp. 1073-1080, 2008.
- [9] H. Sahbi, "A Particular Gaussian Mixture Model For Clustering And Its Application To Image Retrieval", *Soft Computing*, Springer, Vol. 12, No. 7, pp. 667-676, 2008.
- [10] A.R. Robb, "Biomedical Imaging, Visualization, and Analysis", New York, Wiley, 2000.
- [11] M.A. Balafar, A.R. Ramli, S. Mashohor, "Medical Brain Magnetic Resonance Image Segmentation Using Novel Improvement for Expectation Maximizing", *Neurosciences*, Vol. 16, pp. 242-247, 2011.
- [12] M.A. Balafar, A.R. Ramli, S. Mashohor, "Edge-Preserving Clustering Algorithms and their Application for MRI Image Segmentation", *International Multi Conference of Engineers and Computer Scientists*, pp. 17-19, 2010.
- [13] M.A. Balafar, A.R. Ramli, M.I. Saripan, S. Mashohor, R. Mahmud, "Improved Fast Fuzzy C-Mean and its Application in Medical Image Segmentation", *Journal of Circuits, Systems, and Computers*, Vol. 19, pp. 203-214, 2010.
- [14] M.A. Balafar, A.R. Ramli, M.I. Saripan, S. Mashohor, R. Mahmud, "Medical Image Segmentation Using Fuzzy C-Mean (FCM) and User Specified Data", *Journal of Circuits, Systems, and Computers*, Vol. 19, pp. 1-14, 2010.
- [15] W.M. Wells, W.L. Grimson, R. Kikinis, F.A. Jolesz, "Adaptive Segmentation of MRI Data", *IEEE Trans. Med. Imaging*, Vol. 15, pp. 429-42, 1996.
- [16] Y.Y. Zhang, M. Brady, S. Smith, "Segmentation of Brain MR Images through a Hidden Markov Random Field Model and the Expectation Maximization Algorithm", *IEEE Transactions on Medical Imaging*, Vol. 20, No. 1, January 2001.
- [17] H. Tang, et al., "A Vectorial Image Soft Segmentation Method Based on Neighborhood Weighted Gaussian Mixture Model", *Comput. Med. Imaging Graph*, doi:10.1016/j.compmedimag.2009.07.001, 2009.
- [18] H. Gudbjartsson, S. Patz, "The Rician Distribution of Noisy MRI Data", *Magnetic Resonance in Medicine*, Vol. 34, pp. 910-914, 1995.
- [19] BrainWeb, www.bic.mni.mcgill.ca/brainweb/.
- [20] IBSR, www.cma.mgh.harvard.edu/ibsr/.
- [21] A.R.F.D. Silva, "Bayesian Mixture Models of Variable Dimension for Image Segmentation", *Computer Methods and Programs in Biomedicine*, Vol. 94, pp. 1-14, 2009.
- [22] M.N. Ahmed, S.M. Yamany, N. Mohamed, A.A. Farag, T. Moriarty, "A Modified Fuzzy C-Means Algorithm for Bias Field Estimation and Segmentation of MRI Data", *IEEE Trans. Med. Imaging*, Vol. 21, pp. 193-199, 2002.
- [23] W. Cai, S. Chen, D. Zhang, "Fast and Robust Fuzzy C-Means Clustering Algorithms Incorporating Local Information for Image Segmentation", *Pattern Recognition*, Vol. 40, pp. 825-838, 2007.
- [24] L. Szilagyii, Z. Benyo, S.M. Szilagyii, H.S. Adam, "MR Brain Image Segmentation Using an Enhanced Fuzzy C-Means Algorithm", *25th Annual International Conference of IEEE EMBS*, pp. 17-21, 2003.
- [25] J. Wang, J. Kong, Y. Lub, M. Qi, B. Zhang, "A Modified FCM Algorithm for MRI Brain Image Segmentation Sing Both Local and Non-Local Spatial Constraints", *Computerized Med. Imaging and Graphics*, doi:10.1016/j.compmedimag.2008.08.004, 2008.
- [26] P.L. Bazin, D.L. Pham, "Topology Preserving Tissue Classification of Magnetic Resonance Brain Images", *IEEE Transactions on Medical Imaging*, Vol. 26, 2007.
- [27] Y. Zhou, J. Bai, "Atlas Based FC Segmentation and Intensity Nonuniformity Correction Applied to Brain MRI", *IEEE Transactions on Biomedical Engineering*, Vol. 54, pp. 122-129, 2007.
- [28] A.R.F.D. Silva, "A Dirichlet Process Mixture Model for Brain MRI Tissue Classification", *Medical Image Analysis*, Vol. 11, pp. 169-182, 2007.

BIOGRAPHY



Mohammad Ali Balafar was born in Tabriz, Iran, in June 1975. He received the Ph.D. degree in IT in 2010. Currently, he is an Assistant Professor in Department of IT, Faculty of Electrical and Computer Engineering, University of Tabriz, Tabriz, Iran. His research interests are

in artificial intelligence and image processing. He has published 10 journal papers and 4 book chapters.